



Article

Influence of Ceramic Size and Morphology on Interface Bonding Properties of TWIP Steel Matrix Composites Produced by Lost-Foam Casting

Guojin Sun ^{1,*}, Xiaoming Liu ¹, Zhenggui Li ¹ and Qi Wang ²

¹ School of Engineering, Qinghai Institute of Technology, Xining 810016, China; xmlu@qh.it.edu.cn (X.L.); lzkgui@mail.xhu.edu.cn (Z.L.)

² Electrical Engineering Division, Department of Engineering, University of Cambridge, Cambridge CB3 0FA, UK; qw273@cam.ac.uk

* Correspondence: guojinsun@qh.it.edu.cn

Abstract: This study investigated the fabrication and characterization of large ceramic-reinforced TWIP (twinning-induced plasticity) steel matrix composites using the lost-foam casting technique. Various ceramic shapes and sizes, including blocky, flaky, rod-like, and granular forms, were evaluated for their suitability as reinforcement materials. The study found that rod-like and granular ceramics exhibited superior structural integrity and formed strong interfacial bonds with the TWIP steel matrix compared to blocky and flaky ceramics, which suffered from cracking and fragmentation. Detailed microstructural analysis using scanning electron microscopy (SEM) and industrial computed tomography (CT) revealed the mechanisms influencing the composite formation. The results demonstrated that rod-like and granular ceramics are better for reinforcing TWIP steel composites, providing excellent mechanical stability and enhanced performance. This work contributes to the development of advanced composite structures with potential applications in industries requiring high-strength and durable materials.

Keywords: ceramic reinforcement; TWIP steel; lost-foam casting; metal matrix composites



Citation: Sun, G.; Liu, X.; Li, Z.; Wang, Q. Influence of Ceramic Size and Morphology on Interface Bonding Properties of TWIP Steel Matrix Composites Produced by Lost-Foam Casting. *Metals* **2024**, *14*, 1003. <https://doi.org/10.3390/met14091003>

Academic Editors: Tilo Zienert and Christos G. Aneziris

Received: 7 August 2024

Revised: 28 August 2024

Accepted: 30 August 2024

Published: 2 September 2024



Copyright: © 2024 by the authors. Licensee MDPI, Basel, Switzerland. This article is an open access article distributed under the terms and conditions of the Creative Commons Attribution (CC BY) license (<https://creativecommons.org/licenses/by/4.0/>).

1. Introduction

In response to the evolving demands of modern industries driven by societal progress and technological advancements, material requirements have become increasingly stringent [1,2]. Materials are now expected to exhibit not only high strength and hardness but also significant toughness and plasticity. As a result, traditional single-material systems are increasingly inadequate to meet these comprehensive demands. This has spurred urgent research and development of materials that combine superior mechanical properties with exceptional performance [3]. Previous studies have demonstrated the critical role that ceramic reinforcement size, morphology, and distribution play in determining the mechanical properties and interfacial bonding of metal matrix composites. Specifically, Sekaran [4] highlighted how fine ceramic particles can significantly enhance a composite's strength and wear resistance, while other researchers detailed the impact of carbon nanotubes and micron-sized titanium carbide on the thermal expansion of composites [5]. Furthermore, Rajkumar et al. discussed the influence of silicon filler size and concentration on thermal stability and erosion wear resistance of polymer composite [6], and Han et al. provided insights into the optimal processing conditions to achieve uniform ceramic dispersion within the matrix [7,8]. Many studies collectively underscore the importance of precise control over ceramic characteristics in optimizing composite performance, reinforcing the objectives and findings of the present research [9,10].

Unlike aluminum, which is more commonly used due to its lower density and easier processing, steel requires overcoming difficulties such as higher processing temperatures

and potential issues with thermal expansion mismatch. However, once these challenges are managed, steel provides superior mechanical properties and wear resistance, making it a viable option for specific high-performance applications. Historical research on steel-based composites has primarily concentrated on carbide-reinforced and boride-reinforced systems [11,12]. There has been a significant focus on in situ self-generation techniques for fabricating ceramic-reinforced steel matrix composites [13]. These methods aim to incorporate high-hardness particles to produce composites with enhanced overall strength and stiffness. This approach leverages the inherent mechanical advantages of ceramics while capitalizing on the toughness and workability of steel, providing a promising pathway for advanced material applications in demanding environments [14].

Increasing the content of ceramic reinforcements is a key strategy to improve the hardness and wear resistance of steel matrix composites. However, the reinforcement phase cannot be increased indefinitely due to constraints imposed by fabrication techniques and material compatibility. Some scholars have employed the spark plasma sintering (SPS) method to produce TiC-reinforced composites [15]. By incorporating SiC into a stainless steel matrix, they have created composites suitable for high-performance applications such as valve seats and mechanical seals [16]. These materials, when subjected to oil or inert gas quenching, achieve hardness levels exceeding HRC65 and exhibit excellent transverse rupture strength. This makes them suitable for tools and components that must withstand high bending and tensile stresses, while also providing excellent wear resistance and thermal shock stability, ensuring prolonged operational life in demanding environments. Similarly, using the powder metallurgy method, scholars have prepared metal matrix composites with ceramic content exceeding 20%. These composites are embedded in high-alloy steel to fabricate molds, which have demonstrated a lifespan five to ten times longer than molds made from ledeburitic chromium steel [17]. This remarkable durability underscores the benefits of incorporating high-volume ceramic reinforcements. Many findings reveal that the TiC-steel combination offers the best interfacial bonding among various reinforcements [18]. While the addition of ceramic reinforcements significantly improves wear resistance, it also reduces tensile strength, ductility, and impact toughness. These observations highlight the inherent trade-offs involved in optimizing the composition and microstructure of advanced composites to meet specific application requirements.

Various fabrication methods for ceramic-reinforced steel matrix composites have been explored, including spray deposition, powder metallurgy, in-situ reaction, and casting techniques [19]. Each method presents distinct advantages and challenges. Spray deposition allows precise control over the reinforcement volume fraction and maintains good interfacial stability between the reinforcement and matrix. However, high production costs, complex processes, and the need for specialized equipment limit its large-scale application. Powder metallurgy can produce composites with strong matrix–reinforcement bonding but involves complex equipment and processes, resulting in high production costs. Additionally, the tendency for reinforcement particles to agglomerate can lead to non-uniform material properties.

The in-situ reaction method is advantageous due to its simplicity and cost-effectiveness, producing a clean interface with strong bonding between the reinforcement and matrix. However, this method is constrained by a lengthy processing cycle and a limited range of possible reinforcement systems, making it challenging to produce composites with large reinforcement particles, especially when using steel as the matrix material [20]. In contrast, casting techniques, though less effective for composites with small, high-volume fraction ceramic reinforcements due to difficulties in achieving uniform distribution, remain a practical choice for industrial-scale production. While casting with aluminum matrices is relatively straightforward due to aluminum's lower melting point and better wettability on ceramics [21,22], using steel as the matrix introduces complexities such as higher processing temperatures and increased difficulty in maintaining uniform reinforcement distribution. Despite these challenges, casting is still favored for steel matrix composites with moderate to

low reinforcement content due to its simplicity, cost-effectiveness, and broader applicability in industrial contexts.

To address the challenges of brittleness and low ductility in steel matrix composites, employing steels with excellent plastic deformation capabilities as the matrix material is a viable strategy. Twinning-induced plasticity (TWIP) steel, a newly developed material, offers a remarkable combination of high strength and ductility [23,24]. Composed primarily of Fe with 15–30% Mn, TWIP steel features a stable austenitic structure. Under applied external loads, TWIP steel undergoes a mechanical twinning mechanism induced by strain, resulting in significant uniform elongation without necking. This unique behavior imparts exceptional mechanical properties, including elongation rates ranging from 30% to 95% and tensile strengths of 600 to 1924 MPa [25,26]. Furthermore, TWIP steel's ability to absorb impact energy exceeds that of conventional high-strength steels more than twofold, making it an ideal matrix material to mitigate the brittleness of ceramic reinforcements.

Incorporating large-scale ceramic elements, such as rods, plates, or blocks, can further enhance the ceramic reinforcement content. These larger ceramic reinforcements possess extremely high strength and hardness. Combining TWIP steel as the matrix with such centimeter-scale ceramic reinforcements is anticipated to result in composites exhibiting a synergistic combination of properties: the high hardness and strength of the ceramics coupled with the high ductility and toughness of the TWIP steel matrix [27–29]. This innovative composite structure could represent a significant advancement in the field of metal matrix composites, offering a unique blend of superior mechanical characteristics.

Based on these insights, this study aims to investigate the feasibility of fabricating large ceramic-reinforced TWIP steel matrix composites using the lost-foam casting technique. This method is recognized for its ability to achieve complex geometries and high dimensional accuracy while maintaining the integrity of the ceramic reinforcements during the casting process. The research will assess the influence of various ceramic reinforcement shapes and sizes on the composite's overall properties and structural integrity. By analyzing the impact of different reinforcement geometries, the study seeks to provide valuable technical support and empirical data for the design and development of novel ceramic-particle-reinforced steel matrix composites. This research endeavors to bridge gaps in current materials science and demonstrate that lost-foam casting methods can be effectively adapted to produce advanced composites with enhanced mechanical properties, thereby contributing to the broader field of metal matrix composites.

2. Experimental Materials and Methods

2.1. Preparation of Experimental Materials

To investigate the feasibility of fabricating large ceramic-reinforced TWIP steel matrix composites using lost-foam casting method. Various geometries of Si_3N_4 ceramic reinforcements—blocks ($115 \times 40 \times 25$ mm), particles ($\varnothing 10 \times 10$ mm), plates ($40 \times 40 \times 5$ mm), and rods (5×95 mm)—were used in the study. The specific sizes of these reinforcements were selected to evaluate their influence on the interface bonding and mechanical properties of the TWIP steel matrix composites. The ceramic reinforcements used in this study were supplied by Hongyang Fine Ceramics Co., Ltd. (Shenyang, China). Key physical properties of these ceramics are detailed in Table 1. The chosen ceramics were selected for their diverse geometries and sizes, allowing a comprehensive assessment of their effects on the composite's properties.

Table 1. Physical properties of ceramics.

Density (g/cm^3)	Modulus of Elasticity (GPa)	Flexural Strength (MPa)	Compressive Strength (MPa)	Thermal Expansion Coefficient ($10^{-6}/^\circ\text{C}$)
>3.2	>290	>600	>2500	>3.1

For the matrix material, a high-toughness TWIP steel was designed with a composition optimized to enhance the composite's mechanical performance. The chemical composition of the TWIP steel matrix, as presented in Table 2, includes carbon (C), silicon (Si), and manganese (Mn) as the primary alloying elements, with strict control of sulfur (S) and phosphorus (P) impurities to maintain high material purity and prevent deleterious effects on mechanical properties. The high manganese content is particularly crucial for stabilizing the austenitic phase and promoting the twinning-induced plasticity effect, which is central to achieving the desired combination of high strength and ductility in the composite structure.

Table 2. Target chemical composition of TWIP steel matrix (wt%).

C	Si	Mn	S	P	Fe
0.6	0.2	19	<0.002	<0.002	Balance

The TWIP steel matrix was specifically designed to leverage the mechanical twinning mechanism under strain, a characteristic that imparts excellent ductility and high strain hardening rates. This is essential for counterbalancing the brittleness typically associated with ceramic reinforcements, thereby achieving a composite with an optimal balance of hardness, strength, and toughness. The low levels of sulfur and phosphorus are critical to preventing the formation of brittle phases that could compromise the composite's performance, especially under dynamic loading conditions.

By utilizing these materials and carefully controlling their compositions and dimensions, this study aims to explore the interaction between the TWIP steel matrix and the ceramic reinforcements. The goal is to develop a composite structure that not only exhibits the superior hardness and wear resistance characteristic of ceramics but also maintains the high ductility and toughness of TWIP steel. These composites are intended for applications where high strength, toughness, and resistance to extreme corrosive conditions are required.

2.2. Preparation of Lost-Foam Casting Molds

In this study, the lost-foam casting process was employed to fabricate large ceramic-reinforced TWIP steel matrix composites. The procedure involved several key steps to ensure the successful integration of ceramic reinforcements within the TWIP steel matrix.

The process began with cutting a block of expanded polystyrene (EPS) foam, commonly referred to as Styrofoam, into the desired shape to match the TWIP steel matrix model. This foam block served as a template for the subsequent metal casting process. Ceramic reinforcements of various geometries—blocks, particles, plates, and rods—were meticulously arranged on the foam pattern to ensure precise alignment with the intended composite structure. This process involved placing the ceramic reinforcements in specific locations based on their size and shape to optimize their distribution and integration within the mold. In the lost-foam casting process, the foam pattern, now integrated with the ceramic reinforcements, was coated with a refractory material to provide structural support and maintain the mold shape during metal pouring. The primary function of the refractory coating in this technique is to create a stable mold that withstands the thermal and mechanical stresses of the molten metal, rather than preventing metal-foam reactions. The refractory coating ensures that the mold retains its integrity and shape throughout the casting process, which is crucial for achieving the desired composite structure. This coating was dried at 45 °C, a process repeated 2–3 times to achieve sufficient thickness and strength. The fully coated and dried foam pattern was then embedded in a casting sand box, forming the final mold for the casting process. The sand box provided structural support during the casting and helped maintain the shape of the composite.

The overall process is illustrated in Figure 1, depicting the sequential steps involved in preparing the large ceramic-reinforced TWIP steel matrix composite.

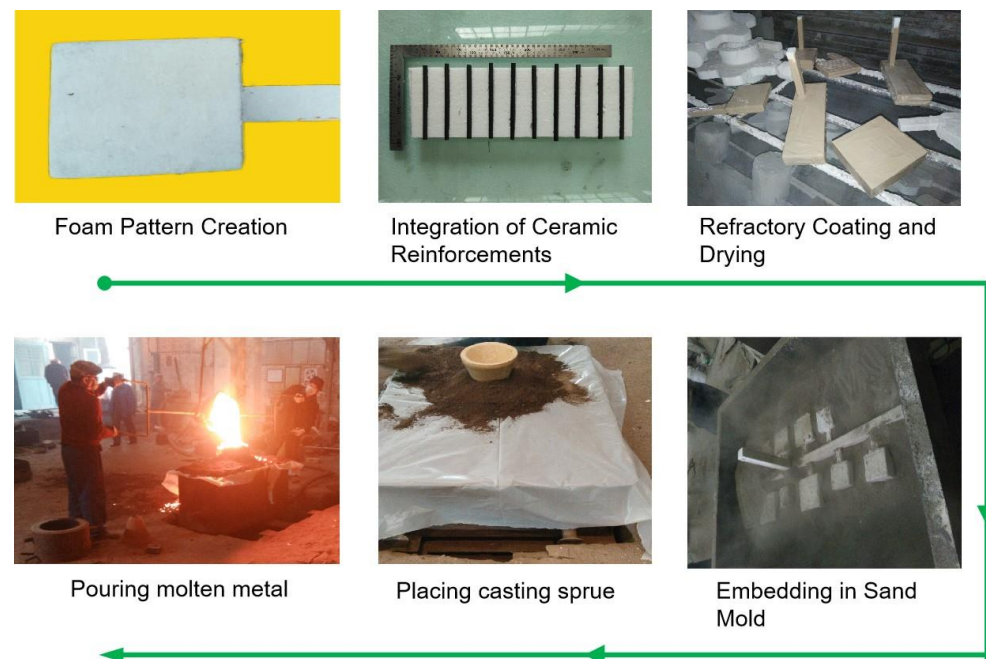


Figure 1. Schematic of the fabrication process for large ceramic-reinforced TWIP steel matrix composites.

The raw materials used for melting the TWIP steel matrix included pure iron, medium carbon ferromanganese, and Q235 steel. The raw materials were provided by Henan Tianyuan Precision Mould Co., Ltd. (Xinxiang, China), and the chemical compositions of these materials are detailed in Table 3.

Table 3. Chemical composition of raw materials for TWIP steel (wt%).

Material	C	Si	Mn	S	P	Fe
Pure Iron	0.01	0.06	0.2	0.012	0.015	Balance
Medium Carbon Ferromanganese	1.7	1.44	75	≤0.0046	≤0.137	Balance
Q235 Steel	0.2~0.3	0.1~0.2	0.17	≤0.04	≤0.04	Balance

The TWIP steel matrix material was melted using a 100 kg medium-frequency induction furnace, manufactured by XinYan Industrial Equipment Co., Ltd. (Shanghai, China). The choice of melting crucible is critical when conducting the melting process in a steel mill. Commonly used crucibles include quartz, ceramic, and graphite. Due to the high melting temperature of TWIP steel, a quartz crucible, known for its excellent high-temperature resistance and corrosion resistance, was selected for melting the TWIP steel matrix. The lost-foam casting process was conducted under vacuum conditions, with a pressure range of 0.015 to 0.02 MPa, to enhance the metal's filling capability and ensure a dense and homogeneous microstructure in the resulting composite structure. During the melting process, pure iron and Q235 steel were first fully melted, followed by the addition of medium carbon ferromanganese. This sequence ensured that the ferromanganese melted completely and integrated well into the steel matrix. A covering agent was added after the complete melting of the ferromanganese to prevent oxidation and loss of manganese. The melt was then held at temperature for 10 min before casting, ensuring that the molten metal was homogenized. The pouring temperature was carefully controlled, with the molten metal being poured at a temperature no lower than 1540 °C to guarantee better flow and filling characteristics. The large ceramic-reinforced TWIP steel matrix composites were successfully prepared using the lost-foam casting method, as shown in Figure 2. The composition of the prepared TWIP steel matrix was analyzed using optical emission spectrometry (OES) (Waltham, MA, USA), and the results are presented in Table 4.



Figure 2. Large fabricated ceramic-reinforced TWIP steel matrix composite samples.

Table 4. Measured chemical composition of TWIP steel matrix (wt%).

C	Si	Mn	S	P	Fe
0.802	0.915	20.45	0.0045	0.075	Balance

As shown in Table 4, the actual contents of carbon and silicon are slightly higher than the designed composition, and the levels of sulfur and phosphorus impurities are also relatively elevated. It can be inferred that by further reducing the carbon content and controlling the levels of sulfur and phosphorus impurities, the toughness and plastic deformation capability of the TWIP steel matrix could be further enhanced. Although there are some fluctuations between the actual and designed chemical compositions, they still fall within the acceptable range for TWIP steel. Since this study focuses on validating the feasibility of ceramic-reinforced TWIP steel fabrication, these variations in chemical composition do not impact the research objectives.

2.3. Evaluation of Ceramic and TWIP Steel Matrix Composite Performance

To evaluate the effectiveness of the composite fabrication and assess the quality of the resulting large ceramic-reinforced TWIP steel matrix composites, a high-performance industrial computed tomography (CT) system supplied by Granpect Company Limited (Beijing, China) was employed. This non-destructive testing method provided detailed tomographic images of the composite samples, allowing an in-depth analysis of the integration between the ceramic reinforcements and the TWIP steel matrix. It also facilitated the identification of any defects formed during the composite preparation process, such as voids, cracks, or improper bonding.

The setup involved positioning the X-ray source and detector at precise distances from the sample: the source was 2.75 m away, while the detector was positioned 3.4 m from the source. This configuration optimized the resolution and accuracy of the CT imaging, ensuring that even subtle details in the composite structure could be captured and analyzed. The experimental setup is illustrated in Figure 3.

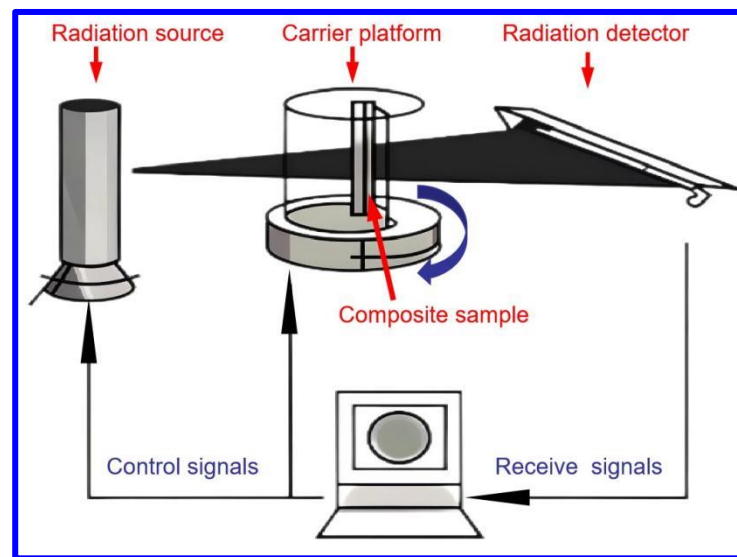


Figure 3. Schematic of the working principle of industrial CT scanning.

For further microstructural analysis, the composite samples were subjected to mechanical processing and wire-cutting to prepare specimens for scanning electron microscopy. A Scanning Electron Microscopy (SEM) analysis was performed using a JEOL JSM-7800F microscope (Akishima, Japan). The analysis was conducted at an acceleration voltage of 10 kV to ensure high-resolution imaging of the microstructural features. The working distance was maintained at approximately 10 mm to achieve optimal image clarity and depth of field. This analysis was crucial for understanding the bonding characteristics at the microscopic level, including the integrity and continuity of the interface, the presence of any interfacial phases, and the overall distribution of the reinforcement within the matrix.

The combination of CT imaging and SEM analysis provided a comprehensive understanding of the composite's internal structure and the quality of the ceramic–matrix bonding. The insights gained from these observations contribute to optimizing the fabrication process, ensuring the production of high-performance composites with minimal defects and superior structural integrity.

3. Results and Discussion

3.1. Fabrication of Ceramic-Reinforced TWIP Steel Matrix Composites

To analyze the effectiveness of the bonding between different ceramic shapes and the TWIP steel matrix, industrial CT was employed for non-destructive testing. The results for plate and block ceramics are illustrated in Figure 4.

Figure 4 presents the industrial CT scan results in different orientations. It is evident that large block ceramics ($115 \times 40 \times 25$ mm) and thin plate ceramics ($40 \times 40 \times 5$ mm) experienced significant cracking during casting. The thin plate ceramics, with a constant thickness of 5 mm but varying surface areas, experienced severe damage in this research. The block ceramics exhibited significant damage at the sharp corners and developed numerous cracks on the surface. These cracks compromised the integrity of the ceramic reinforcements, as seen in Figure 4a,b, rendering them ineffective in strengthening the matrix. The fragmented ceramics not only failed to enhance the matrix but also potentially degraded its properties. Furthermore, as shown in Figure 4b, substantial voids formed at the interface between the large ceramics and the matrix during the casting process, preventing a strong bond. This suggests that large block and thin plate ceramics are prone to cracking and porosity formation during the composite fabrication process, making them unsuitable as reinforcements for large TWIP steel matrix composites.

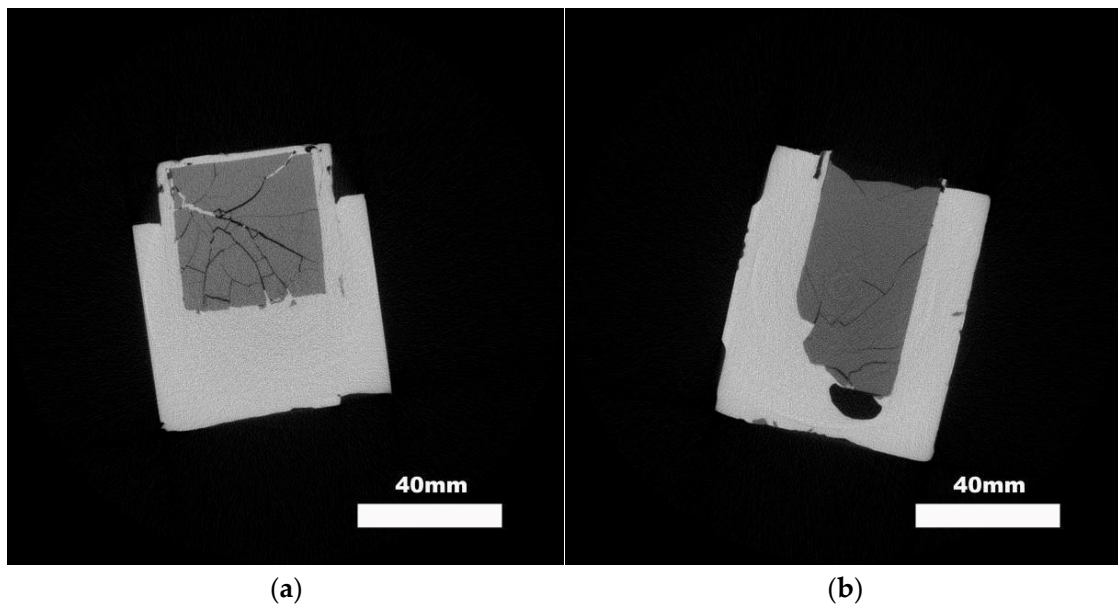


Figure 4. Industrial CT results for plate and block ceramic-reinforced TWIP steel matrix composites. (a) Internal structure of plate ceramic reinforcement; (b) internal structure of block ceramic reinforcement.

In contrast, the results for rod ceramics ($\varphi 5 \times 95$ mm) and granular ceramics ($\varphi 10 \times 10$ mm) are shown in Figure 5.

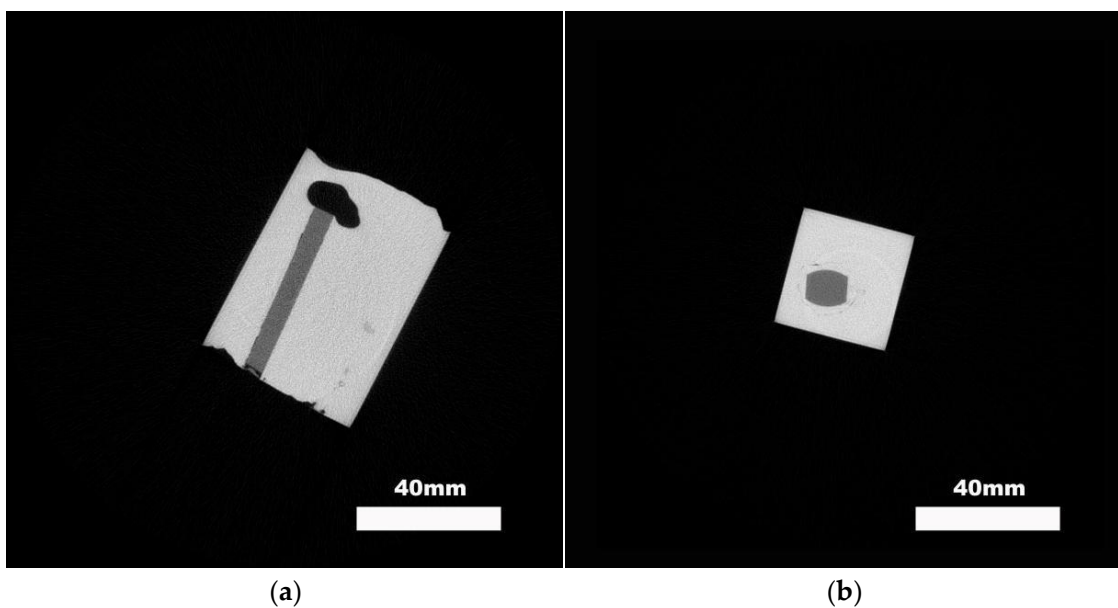


Figure 5. Industrial CT results for rod and particle ceramic-reinforced TWIP steel matrix composites. (a) Internal structure of rod ceramic reinforcement; (b) internal structure of granular ceramic reinforcement.

Figure 5 demonstrates that when uniformly cross-sectioned rod ceramics ($\varphi 5 \times 95$ mm) and granular ceramics ($\varphi 10 \times 10$ mm) were used, no visible cracks or fragmentation occurred. The ceramic reinforcements maintained their integrity, and there was good bonding between the ceramics and the TWIP steel matrix. The interface quality was significantly better compared to that of block and plate ceramics. This indicates that the rod and granular ceramics used in this research, with their symmetrical cross-sections, can form a strong and cohesive bond with the TWIP steel matrix. Due to their uniform or circular

cross-sections, these rod and granular ceramics experience reduced stress concentration during bonding with the TWIP steel, leading to a lower tendency toward crack formation and making them suitable for fabricating large ceramic-reinforced TWIP steel matrix composite structures.

It is important to note that the observed porosity defects in Figures 4b and 5a are common issues in the lost-foam casting process. These defects, resulting from the casting phase, can be minimized through process optimization, such as adjusting the gating system and ceramic positioning. Ensuring the correct size and shape of the ceramic reinforcements is crucial for maintaining the structural integrity and preventing cracks. Despite the presence of casting porosity in both Figures 4b and 5a, the rod-shaped ceramics did not exhibit cracks and showed a strong bond with the TWIP steel matrix. These observations highlight the significance of choosing appropriately shaped and sized ceramic reinforcements to ensure the structural integrity and mechanical performance of the composites. Based on the performance observed in this study, rod and spherical ceramics, due to their more uniform geometrical features, are better suited for creating a robust composite with TWIP steel compared to plate and block ceramics. This approach offers a promising solution for advanced material applications that require a balance of strength and toughness.

3.2. Interfacial Morphology Analysis of Large Ceramic-Reinforced TWIP Steel Matrix Composites

To investigate the interfacial bonding and microstructural characteristics of the granular ceramics with the TWIP steel matrix, samples of $\phi 10 \times 10$ mm granular ceramic-reinforced TWIP steel composites were sectioned and examined using scanning electron microscopy (SEM). The results are shown in Figure 6.

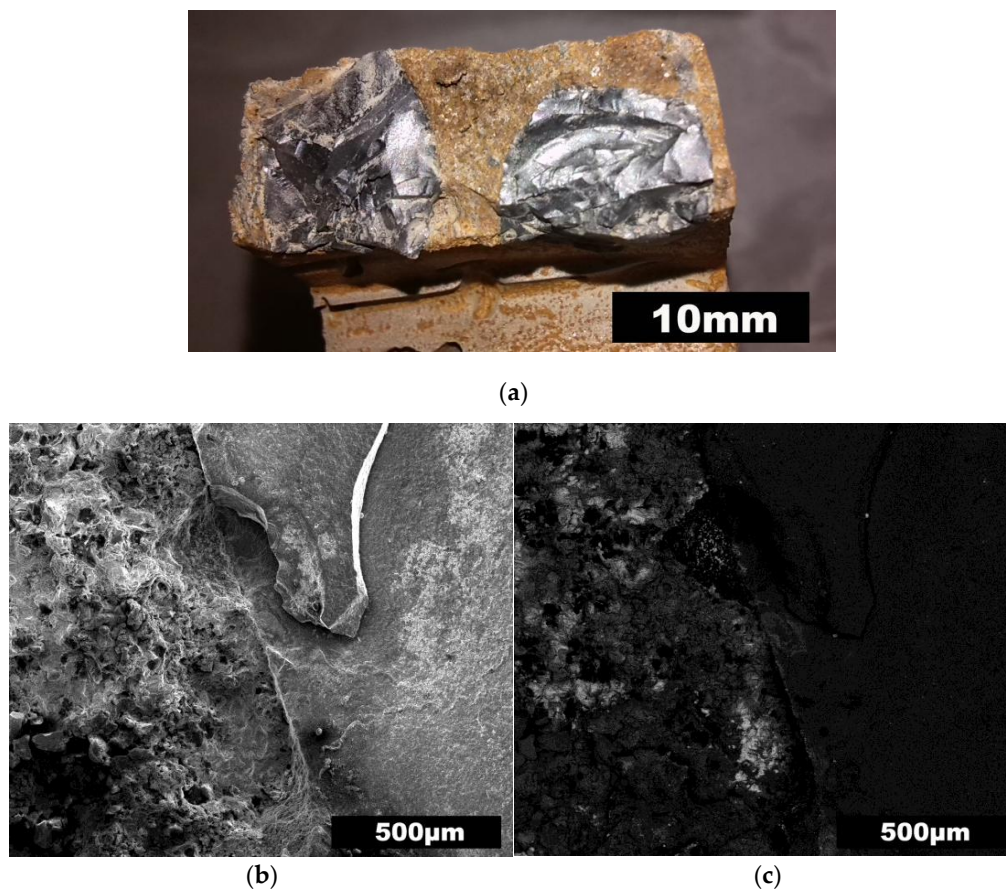


Figure 6. Microstructural observations at the interface of large ceramics and the TWIP steel matrix. (a) Macroscopic interfacial bonding; (b) secondary electron SEM morphology; (c) backscattered electron SEM morphology.

In Figure 6a, the macroscopic observation reveals that the ceramic are tightly embedded in the surrounding TWIP matrix, indicating a robust macroscopic bond. The SEM images further support this observation. As seen in Figure 6b, the secondary electron SEM morphology shows a well-defined and intimate bonding between the ceramic reinforcement and the TWIP steel matrix at the microscopic level. The tight integration of the ceramics with the metal matrix suggests a strong interfacial bond, essential for effective load transfer and composite performance. Notably, the cracks observed in the right side of the ceramic particle in Figure 6b are attributed to the sample preparation process and not the casting process, indicating the robustness of the interface under the actual manufacturing conditions. The backscattered electron SEM morphology in Figure 6c provides additional insight into the compositional differences at the interface. This image clearly delineates the ceramic and the TWIP steel matrix, showing a distinct interface region where the two phases interact.

To further understand the compositional characteristics at the interface, elemental line scans were performed across the ceramic and matrix phases. The results are presented in Figure 7.

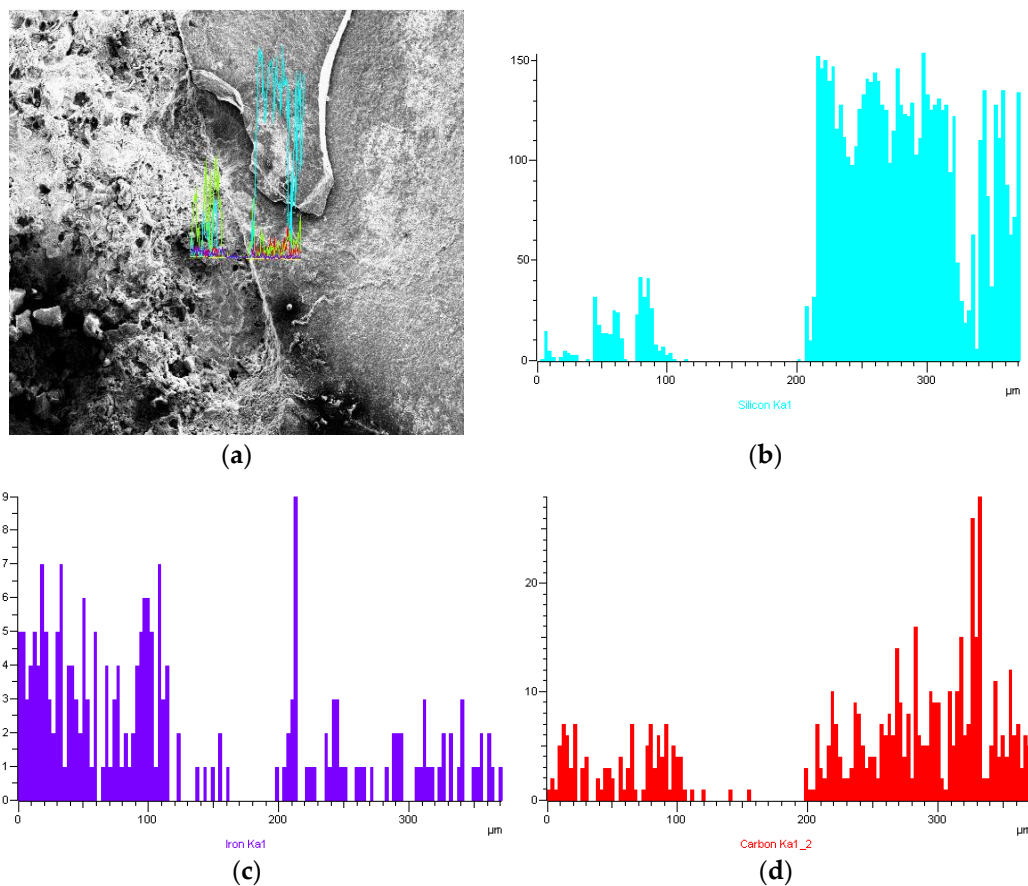


Figure 7. Elemental line distribution at the ceramic and TWIP steel matrix interface. (a) SEM microstructure of interface; (b) Si distribution at the interface; (c) Fe distribution at the interface; (d) C distribution at the interface.

The elemental line scans in Figure 7 reveal a distinct transition zone where the ceramic and the TWIP steel matrix meet. The distributions of Fe, C, and Si across the interface indicate some degree of elemental diffusion, suggesting the formation of a transitional layer. This diffusion can enhance the interfacial bonding strength and contribute to a smoother stress transfer between the ceramic and metallic phases. The presence of a transitional layer, characterized by gradual changes in elemental composition, further confirms the good microstructural compatibility and bonding at the interface.

The SEM and elemental analysis indicate that the $\phi 10 \times 10$ mm granular ceramics form a strong and cohesive interface with the TWIP steel matrix. This is crucial for achieving the desired mechanical properties in the composite, such as improved strength and toughness. The study indicates that the selected ceramic particles have potential for reinforcing the TWIP steel matrix. However, to definitively validate their effectiveness and suitability for applications requiring advanced material performance, further mechanical property testing and analysis would be necessary to corroborate the reinforcement effects observed in the SEM imaging.

3.3. Analysis of the Composite Process for Large Ceramics with TWIP Matrix

The analysis of the composite process indicates that ceramics with more uniform cross-sectional dimensions, such as rod-shaped and spherical ceramics, are more suitable as reinforcement materials for TWIP steel matrix composites. In contrast, large block-shaped and plate-like ceramics, which exhibit significant differences in cross-sectional dimensions, are prone to fragmentation and cracking, hindering their effective integration with the TWIP steel matrix. This behavior is closely related to the casting performance of the matrix and the stress state of the ceramic reinforcement during the casting process.

One critical factor affecting the composite process is the temperature gradient between the molten steel and the ceramic reinforcement. When molten steel comes into contact with the ceramic, a significant temperature drop occurs due to the high thermal conductivity of the ceramics. This temperature change can significantly influence the formation and quality of the composite structure. For smaller ceramics, such as $\phi 10 \times 10$ mm granular ceramics and $\phi 5 \times 95$ mm rod-shaped ceramics, the molten steel's temperature drop is relatively small upon contact. The subsequent heat transfer from the molten steel maintains sufficient fluidity and feeding capacity, ensuring a good bond between the ceramic and the matrix material. In contrast, when larger ceramic reinforcements come into contact with the molten steel, the temperature of the steel melt decreases. The ceramics themselves, initially at room temperature, experience a temperature rise. The observed crackling in the ceramic plates is likely due to uneven temperature distribution across the ceramic sections—where the temperature increase is more pronounced at the corners compared to the center—and due to increased stress concentration in non-rounded geometries. Despite subsequent heat conduction from the molten steel, the rapid temperature decrease impedes the fluidity and feeding of the molten steel, making defect formation more likely. Therefore, from the perspective of the effect of ceramics on the molten steel's fluidity and feeding capacity, smaller ceramics such as $\phi 10 \times 10$ mm granular ceramics and $\phi 5 \times 95$ mm rod-shaped ceramics are the better choices.

During the lost-foam casting process, ceramic reinforcements are subjected to various stresses, including thermal stress, shrinkage stress from the molten steel, and internal stress. The magnitude of these stresses depends on the ceramic's surface area. Ceramics with larger differences in cross-sectional dimensions experience uneven force distribution, increasing the likelihood of cracking under unbalanced external forces. When the ceramic reinforcements are $\phi 5 \times 95$ mm rods or $\phi 10 \times 10$ mm granular ceramics, the uniformity in cross-sectional shape ensures that the molten metal almost instantly and uniformly envelops the ceramic particles during pouring. Consequently, the ceramics experience uniform stress, preventing crack formation and maintaining the integrity of the ceramic reinforcement.

In essence, the findings underscore the critical importance of selecting ceramic reinforcement materials with uniform cross-sectional dimensions to achieve a stable and defect-free composite process. The $\phi 10 \times 10$ mm granular ceramics and $\phi 5 \times 95$ mm rod-shaped ceramics are expected to contribute to the enhancement of the composite structure's mechanical properties. However, it is important to note that this expectation is based on theoretical predictions rather than empirical testing. The actual improvement in mechanical properties will need to be confirmed through rigorous testing and validation.

4. Conclusions

In this study, we have successfully demonstrated the feasibility of producing large ceramic-reinforced TWIP steel matrix composites using the lost-foam casting technique. The research investigated various ceramic shapes and sizes, including blocky, flaky, rod-like, and granular forms, to determine their suitability as reinforcement materials. Key findings and insights from this study are as follows:

1. It was observed that blocky (115 × 40 × 25 mm) and flaky (40 × 40 × 5 mm) ceramic reinforcements experienced significant cracking and fragmentation during the lost-foam casting process. These defects compromised the integrity of the composite and diminished the reinforcement's effectiveness. In contrast, rod-like ($\phi 5 \times 95$ mm) and granular ($\phi 10 \times 10$ mm) ceramics demonstrated superior compatibility with the TWIP steel matrix. They maintained their structural integrity, resulting in a robust and cohesive composite structure.
2. The SEM and CT analyses revealed that rod-like and granular ceramics formed favorable interfacial bonding with the TWIP matrix. The microstructural examination indicated that the ceramics were well embedded within the matrix, with minimal interfacial defects.
3. Smaller, more uniformly shaped ceramics, such as rods and granules, allowed better heat dissipation and reduced thermal stress. This led to fewer defects and better overall material properties. The findings underscore the importance of controlling ceramic size and shape to minimize thermal and mechanical stresses during lost-foam casting.
4. Based on the comprehensive analysis, rod-like and granular ceramics emerged as the better choices for reinforcing large TWIP steel matrix composites.

Author Contributions: Conceptualization, G.S.; Data Curation, G.S., X.L. and Q.W.; Formal Analysis, G.S., X.L., Z.L. and Q.W.; Investigation, G.S., X.L., Z.L. and Q.W.; Methodology, G.S., X.L., Z.L. and Q.W.; Supervision, G.S. and Z.L.; Writing—Original Draft, G.S. and X.L.; Writing—Review and Editing, G.S. and Z.L. All authors have read and agreed to the published version of the manuscript.

Funding: The authors acknowledge financial support from the Kunlun Talent Project of Qinghai Province, People's Republic of China (2023-QLGKLYCZX-034).

Data Availability Statement: The data presented in this study are available on request from the corresponding author due to privacy.

Conflicts of Interest: The authors declare no conflicts of interest.

References

1. Lee, H.; Lee, S.; Ryu, S. Advancements and Challenges of Micromechanics-based Homogenization for the Short Fiber Reinforced Composites. *Multiscale Sci. Eng.* **2023**, *5*, 133–146. [[CrossRef](#)]
2. Alhmoudi, A.; Sheikh-Ahmad, J.; Almaskari, F.; Bojanampati, S. Joining of polymer to metal using material extrusion additive manufacturing. *Int. J. Adv. Manuf. Technol.* **2023**, *129*, 3303–3319. [[CrossRef](#)]
3. Sethi, D.; Acharya, U.; Kumar, S.; Shekhar, S.; Roy, B.S. Effect of Reinforcement Particles on Friction Stir Welded Joints with Scarf Configuration: An Approach to Achieve High Strength Joints. *Silicon* **2022**, *14*, 6847–6860. [[CrossRef](#)]
4. Sekaran, P.R.; Ramakrishnan, H.; Venkatesh, R.; Nithya, A. Mechanical and Physical Characterization Studies of Nano Ceramic Reinforced Al–Mg Hybrid Nanocomposites. *Silicon* **2023**, *15*, 4555–4567. [[CrossRef](#)]
5. Nyanor, P.; El-Kady, O.; Yehia, H.M.; Hamada, A.S.; Hassan, M.A. Effect of Bimodal-Sized Hybrid TiC–CNT Reinforcement on the Mechanical Properties and Coefficient of Thermal Expansion of Aluminium Matrix Composites. *Met. Mater. Int.* **2021**, *27*, 753–766. [[CrossRef](#)]
6. Rajkumar, K.; Nambiraj, K.M.; Ramraji, K.; Khan, B.S.H. Influence of silicon filler size and concentration on thermal stability and erosion wear resistance of polymer composite. *Silicon* **2022**, *14*, 9595–9608. [[CrossRef](#)]
7. Han, Y.; Liu, J.; Wang, Q.; Lin, C.; Wang, E.; Wu, W.; Zhang, M. Effect of volume fraction ratio of Ti to Al₃Ti on mechanical and tribological performances of the in situ Ti–Al₃Ti core–shell structured particle reinforced Al matrix composite. *J. Mater. Res.* **2022**, *37*, 3695–3707. [[CrossRef](#)]
8. Bhardwaj, A.R.; Vaidya, A.M.; Meshram, P.D.; Bandhu, D. Machining behavior investigation of aluminium metal matrix composite reinforced with TiC particulates. *Int. J. Interact. Des. Manuf.* **2024**, *18*, 2911–2925. [[CrossRef](#)]

9. Hwang, J.-I.; Kim, S.H.; Heo, Y.-U.; Kim, D.H.; Hwang, K.-C.; Suh, D.-W. Tempering Behavior of TiC-Reinforced SKD11 Steel Matrix Composite. *Met. Mater. Int.* **2018**, *24*, 644–651. [[CrossRef](#)]
10. Kim, S.H.; Kim, D.H.; Hwang, K.-C.; Lee, S.-K.; Hong, H.U.; Suh, D.-W. Heat treatment response of TiC-reinforced steel matrix composite. *Met. Mater. Int.* **2016**, *22*, 935–941. [[CrossRef](#)]
11. Chen, P.-H.; Li, Y.-B.; Li, R.-Q.; Jiang, R.-P.; Zeng, S.-S.; Li, X.-Q. Microstructure, mechanical properties, and wear resistance of VC_p-reinforced Fe-matrix composites treated by Q&P process. *Int. J. Miner. Met. Mater.* **2018**, *25*, 1060–1069. [[CrossRef](#)]
12. Sui, Y.; Han, L.; Jiang, Y.; Li, Z.; Shan, Q. Effects of Ni60WC25 powder content on the microstructure and wear properties of WC_p reinforced surface metal matrix composites. *Trans. Indian Inst. Met.* **2018**, *71*, 2415–2422. [[CrossRef](#)]
13. Kračun, A.; Jenko, D.; Godec, M.; Savilov, S.V.; Prieto, G.; Tuckart, W.; Podgornik, B. Nanoparticles Reinforcement for the Improved Strength and High-Temperature Wear Resistance of Mn-Cr Steel. *Met. Mater. Trans. A* **2018**, *49*, 5683–5694. [[CrossRef](#)]
14. Zafar, H.M.N.; Nair, F. Fabrication and Microscale Characterization of Iron Matrix Composite Wires Reinforced by in situ Synthesized Iron Boride Phases. *Arab. J. Sci. Eng.* **2023**, *48*, 3909–3930. [[CrossRef](#)]
15. Aslam, M.; Chandan, G.K.; Kanchan, B.K. Development of SiC Ceramic Reinforced Composite Interlayer Cladding with AISI304 Stainless Steel Wire on Low Carbon Steel Substrate Using TIG Cladding Process. *Silicon* **2023**, *15*, 7733–7743. [[CrossRef](#)]
16. Sule, R.; Bayode, B.L.; Obadele, B.A.; Asante, J.K.O.; Olubambi, P.A.; Falodun, O.E. Densification and wear behavior of Cu-TiC composites via spark plasma sintering in situ degassing. *Int. J. Adv. Manuf. Technol.* **2022**, *123*, 2415–2426. [[CrossRef](#)]
17. Venkatesh, V.S.S.; Prasad, K.; Patnaik, L. Effect of SiC and TiC Reinforcements on the Mechanical Properties of ZrB₂-SiC-TiC Hybrid Composite Fabricated Through Spark Plasma Sintering. *Silicon* **2023**, *15*, 3339–3351. [[CrossRef](#)]
18. Aghajani, S.; Pouyafar, V.; Meshkabadi, R.; Volinsky, A.A.; Bolouri, A. Mechanical characterization of high volume fraction Al7075-Al₂O₃ composite fabricated by semisolid powder processing. *Int. J. Adv. Manuf. Technol.* **2023**, *125*, 2569–2580. [[CrossRef](#)]
19. Tong, Z.; Shao, W.; He, C.; He, D. Microstructure and wear resistance of in situ TiC-reinforced low-chromium iron-based hardfacing alloys. *Weld. World* **2024**, *68*, 605–620. [[CrossRef](#)]
20. Lakshmikanth, B.; Jesudas, T. Influence of Stainless Steel Short Fibres as Reinforcements in Enhancing the Performance of Aluminium 7075 Alloy Matrix Composites. *Trans. Indian Inst. Met.* **2024**, *77*, 495–501. [[CrossRef](#)]
21. Shavnev, A.A.; Kurbatkina, E.I.; Nyafkin, A.N.; Kosolapov, D.V. Fabrication Technologies of a Dispersion-Reinforced Metallic Composite Material Based on an Aluminum Alloy—Review. *Inorg. Mater. Appl. Res.* **2023**, *14*, 76–80. [[CrossRef](#)]
22. Dong, T.-S.; Liu, J.-H.; Fang, Q.; Li, G.-L.; Zhang, J.-J. High strength bimetallic composite material fabricated by electros slag casting and characteristics of its composite interface. *China Foundry* **2016**, *13*, 389–395. [[CrossRef](#)]
23. Binesh, F.; Zamani, J.; Ghiasvand, M. Ordered Structure Composite Metal Foams Produced by Casting. *Int. J. Met.* **2018**, *12*, 89–96. [[CrossRef](#)]
24. Sohn, S.S.; Song, H.; Jo, M.C.; Song, T.; Kim, H.S.; Lee, S. Novel 1.5 GPa-strength with 50%-ductility by transformation-induced plasticity of non-recrystallized austenite in duplex steels. *Sci. Rep.* **2017**, *7*, 1255. [[CrossRef](#)]
25. Wang, Y.-N.; Yang, J.; Wang, R.-Z.; Xin, X.-L.; Xu, L.-Y. Effects of Non-metallic Inclusions on Hot Ductility of High Manganese TWIP Steels Containing Different Aluminum Contents. *Met. Mater. Trans. B* **2016**, *47*, 1697–1712. [[CrossRef](#)]
26. Lapovok, R.; Berner, A.; Bisht, A.; Acharya, S.; Vahid, A.; Rabkin, E. Strain-induced solid-state coating of TWIP steel sheets with zinc. *J. Mater. Sci.* **2024**, *59*, 5538–5557. [[CrossRef](#)]
27. Lv, W.; Gu, Y.; Huang, Y.; Cai, G.; Misra, R.D.K. An Experimental Investigation on Microstructure and Mechanical Property of Asymmetric Warm-Rolled Fe-27Mn-3Si-4Al TWIP Steel. *J. Mater. Eng. Perform.* **2023**, *32*, 6704–6716. [[CrossRef](#)]
28. Cai, Z.; Wang, S.; Zhou, Y.; Dong, J.; Ma, L.; Liu, S. Influence of aging treatment on mechanical properties and wear resistance of medium manganese steel reinforced with Ti(C,N) particles. *Friction* **2023**, *11*, 2059–2072. [[CrossRef](#)]
29. Vidilli, A.L.; Coury, F.G.; Gonzalez, G.; Otani, L.B.; Amigó, V.; Bolfarini, C. Tailoring the Microstructure and Properties of Reinforced FeMnAlC Composites by In-Situ TiB₂-TiC-M₂B Formation. *Met. Mater. Trans. A* **2024**, *55*, 101–117. [[CrossRef](#)]

Disclaimer/Publisher’s Note: The statements, opinions and data contained in all publications are solely those of the individual author(s) and contributor(s) and not of MDPI and/or the editor(s). MDPI and/or the editor(s) disclaim responsibility for any injury to people or property resulting from any ideas, methods, instructions or products referred to in the content.